Metadata of the article that will be visualized in OnlineFirst

ArticleTitle	Towards a green and cost-effective synthesis of polyanionic cathodes: comparative electrochemical behaviour of LiFePO$_4$/C, Li$_2$FeP$_2$O$_7$/C and Li$_2$FeSiO$_4$/C synthesized using methylcellulose matrix
Article Sub-Title	
Article CopyRight	Indian Academy of Sciences (This will be the copyright line in the final PDF)
Journal Name	Bulletin of Materials Science

Corresponding Author		
	Family Name	**Milović**
	Particle	
	Given Name	**Miloš**
	Suffix	
	Division	
	Organization	Institute of Technical Sciences of SASA
	Address	Belgrade, Serbia
	Phone	
	Fax	
	Email	milos.milovic@itn.sanu.ac.rs
	URL	
	ORCID	http://orcid.org/0000-0002-5957-1399
Author		
	Family Name	**Jugović**
	Particle	
	Given Name	**Dragana**
	Suffix	
	Division	
	Organization	Institute of Technical Sciences of SASA
	Address	Belgrade, Serbia
	Phone	
	Fax	
	Email	
	URL	
	ORCID	
Author		
	Family Name	**Vujković**
	Particle	
	Given Name	**Milica**
	Suffix	
	Division	Faculty of Physical Chemistry
	Organization	University of Belgrade
	Address	Belgrade, Serbia
	Phone	
	Fax	
	Email	

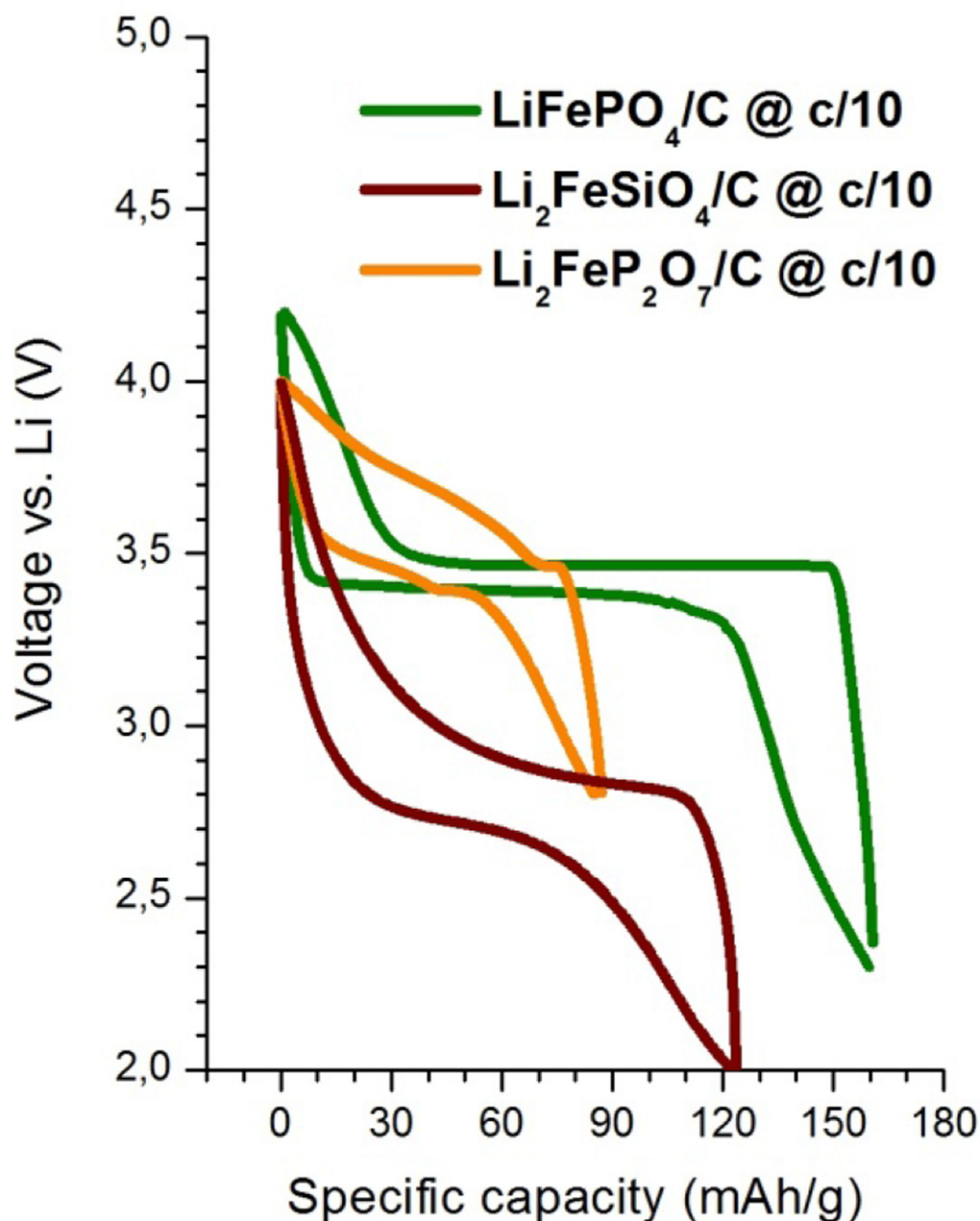| | URL | |
	ORCID	
Author	Family Name	**Kuzmanović**
	Particle	
	Given Name	**Maja**
	Suffix	
	Division	
	Organization	Institute of Technical Sciences of SASA
	Address	Belgrade, Serbia
	Phone	
	Fax	
	Email	
	URL	
	ORCID	
Author	Family Name	**Mraković**
	Particle	
	Given Name	**Ana**
	Suffix	
	Division	Vinča Institute of Nuclear Sciences—National Institute of the Republic of Serbia
	Organization	University of Belgrade
	Address	Belgrade, Serbia
	Phone	
	Fax	
	Email	
	URL	
	ORCID	
Author	Family Name	**Mitrić**
	Particle	
	Given Name	**Miodrag**
	Suffix	
	Division	Vinča Institute of Nuclear Sciences—National Institute of the Republic of Serbia
	Organization	University of Belgrade
	Address	Belgrade, Serbia
	Phone	
	Fax	
	Email	
	URL	
	ORCID	

| Abstract | The polyanion cathodes for Li-ion batteries, namely LiFePO$_4$, Li$_2$FeP$_2$O$_7$ and Li$_2$FeSiO$_4$, were synthesized by very short high-temperature treatment (approximately several minutes) and subsequent quenching. Methylcellulose—a polymer with thermally driven water solubility—was used as the medium in which the |

precursor solutions were dispersed prior to high temperature treatment. The methylcellulose pyrolytically decomposes to carbon, thus producing the polyanion material/carbon composites of $LiFePO_4/C$, $Li_2FeP_2O_7/C$ and Li_2FeSiO_4/C. The obtained powders have reduced crystallinity and significant microstructural characteristics: low crystallite size and notable microstrain. They exhibit stable electrochemical performances in both aqueous and organic electrolyte. The broadening of existing peaks in cyclic voltammetry and/or the emergence of new broad peaks was attributed to the presence of the amorphous phase in the samples. In galvanostatic charge–discharge tests, the materials provided high capacities at low current densities, while the highest rate performance was demonstrated by olivine-phosphate when compared to the other two materials.

Graphical abstract:

MO1:

.

Metadata of the article that will be visualized in OnlineAlone

Graphical abstract:
MO1:

.

Towards a green and cost-effective synthesis of polyanionic cathodes: comparative electrochemical behaviour of LiFePO$_4$/C, Li$_2$FeP$_2$O$_7$/C and Li$_2$FeSiO$_4$/C synthesized using methylcellulose matrix

MILOŠ MILOVIĆ[1],* , **DRAGANA JUGOVIĆ[1], MILICA VUJKOVIĆ[2], MAJA KUZMANOVIĆ[1], ANA MRAKOVIĆ[3] and MIODRAG MITRIĆ[3]**

[1] Institute of Technical Sciences of SASA, Belgrade, Serbia
[2] Faculty of Physical Chemistry, University of Belgrade, Belgrade, Serbia
[3] Vinča Institute of Nuclear Sciences—National Institute of the Republic of Serbia, University of Belgrade, Belgrade, Serbia
*Author for correspondence (milos.milovic@itn.sanu.ac.rs)

Abstract. The polyanion cathodes for Li-ion batteries, namely LiFePO$_4$, Li$_2$FeP$_2$O$_7$ and Li$_2$FeSiO$_4$, were synthesized by very short high-temperature treatment (approximately several minutes) and subsequent quenching. Methylcellulose—a polymer with thermally driven water solubility—was used as the medium in which the precursor solutions were dispersed prior to high temperature treatment. The methylcellulose pyrolytically decomposes to carbon, thus producing the polyanion material/carbon composites of LiFePO$_4$/C, Li$_2$FeP$_2$O$_7$/C and Li$_2$FeSiO$_4$/C. The obtained powders have reduced crystallinity and significant microstructural characteristics: low crystallite size and notable microstrain. They exhibit stable electrochemical performances in both aqueous and organic electrolyte. The broadening of existing peaks in cyclic voltammetry and/or the emergence of new broad peaks was attributed to the presence of the amorphous phase in the samples. In galvanostatic charge–discharge tests, the materials provided high capacities at low current densities, while the highest rate performance was demonstrated by olivine-phosphate when compared to the other two materials.

Keywords. ~~Li-ion battery;~~ polyanion cathodes; LiFePO$_4$; Li$_2$FeP$_2$O$_7$; Li$_2$FeSiO$_4$; methylcellulose; quenching.

1. Introduction

Polyanion cathode materials for Li-ion batteries offer the advantage of higher safety and higher voltage values in comparison to the oxide cathodes with the same M$^{x+/(x+1)+}$ redox pair [1]. Both higher voltage and higher stability come from strong covalent bonding within the polyanion units and these inherent characteristics have promoted investigation of different polyanion compounds: phosphates (PO$_4^{3-}$ polyanion group), pyrophosphates (P$_2$O$_7^{4-}$), silicates (SiO$_4^{4-}$) and others. Among them, the iron-based compounds appear attractive, as Fe is abundant, inexpensive and less toxic than Co, Ni or Mn. LiFePO$_4$ has gained worldwide fame, thanks to its outstanding electrochemical features [2], and become the most widely studied cathode material for Li rechargeable batteries. On the other hand, Li$_2$FeP$_2$O$_7$ and Li$_2$FeSiO$_4$ attracted interest due to the possibility of extraction/insertion of two lithium ions per formula unit, which would lead eventually to higher storage capacities [3, 4].

The rigid structure of polyanion compounds provides cycle stability on the one side but deteriorates ionic diffusion on the other; also, the insertion of polyanion units between FeO$_n$ polyhedrons impedes electron transfer among Fe centres in the lattice [5]. As a result, unlike oxide-based cathodes, polyanion cathodes suffer considerably from the low conductivity (both ionic and electronic), which significantly limits their rate performance and therefore application in high power devices. To overcome this, for some researchers, it seemed tempting to induce a structural degradation of the polyanionic framework, to produce a disordered or defective phase and to investigate the electrochemical response. Zhang *et al* [6] offered the strategy of disorder/order engineering to improve the Li-ion battery anode performances. Xiong *et al* [7] reported the enhanced cathode storage performance of NaFePO$_4$ by mechanochemically induced disorder. Similarly, the activation of β-LiFePO$_4$ was achieved by optimized disordering via ball milling route [8]. The defective phase of olivine LiFePO$_4$ prepared at low temperature [9] or under oxidizing

conditions [10] can result in a completely new electro-chemical signature (monophasic behaviour). Density functional theory calculations suggest that tailoring native defects through a defect-controlled synthesis or post-synthetic treatment can enhance the electrical conductivity of $LiFePO_4$ [11]. The most common defect for $LiFePO_4$ is an anti-site defect, where Li and Fe ions exchange their positions. While its presence hinders the performances of $LiFePO_4$ through the obstruction of Li channel [12], high concentration of anti-sites in Li_2FeSiO_4 or $Li_2FeP_2O_7$ may provide the additional transfer between Li layers [13, 14] and also reduce stress during cycling [15].

This study aimed to synthesize polyanion powders of $LiFePO_4$, $Li_2FeP_2O_7$ and Li_2FeSiO_4 with reduced crystallinity. Inspired by the previous work on the subject, we utilized a method that consists of short high-temperature treatment of the precursors dispersed in a methylcellulose matrix and subsequent quenching. The interval of high temperature treatment–which usually takes several hours to obtain the above-mentioned polyanion phases [2–4, 13, 14, 16]—is reduced to several minutes. The usage of methylcellulose (or other cellulose ethers) is known in the literature for the structure control during ceramic processing [17, 18], but seldom for the synthesis of polyanion cathodes [19]. Being water-soluble, non-toxic and inexpensive (note that cellulose is the most abundant polymer on Earth), the methylcellulose proved its worth as a carbon source in our previous investigations on electrical properties of the composites [20, 21]. The method that was originally developed for Li_2FeSiO_4 [21] is now re-optimized for the group of polyanion cathode materials. The details of the chemical and technical procedures, as well as structural/microstructural examination and a comparison of their electrochemical properties, are given in the following text.

## 2. Experimental

The synthetic procedure consists of two basic steps: (1) precursor preparation in a methylcellulose polymer matrix and (2) short dwell at high temperature. All technical information regarding the chemicals and synthetic conditions that were used are given in table 1. In the first step, stoichiometric amounts of precursor compounds were dissolved in water and mixed with the previously prepared methylcellulose solution. The methylcellulose to inorganic precursor components mass ratio was kept the same (≈ 0.2) for all the three samples (the ratio value corresponds to the value from the sample with the highest content of carbon in [21]). The solution was stirred at ~ 70 °C until gel was formed. The methylcellulose is a derivative of cellulose with the superb solubility properties in aqueous media. Unlike cellulose, the methylcellulose is a water-soluble polymer with an ability to gel upon heating and reversibly liquefy upon cooling [22], due to the hydrophobic interaction between molecules containing methoxyl groups (figure 1).

Table 1. Summary of synthesis conditions.

Sample	Starting compounds	Pre-treatment	Thermal treatment
$LiFePO_4$/C	$FeSO_4 \cdot 7H_2O$ (Sigma-Aldrich, $\geq$ 99.0%), LiH_2PO_4 (Sigma-Aldrich, $\geq$ 99.0%) Methylcellulose (Dow, Methocel™, A4C)	Sol–gel; magnetic stirring for several hours at 60–70 °C until all water evaporated	700°C, dwell time: 10min; flowing Ar + 5%H_2 (flow rate $\sim$ 0.1 dm³ min⁻¹)
$Li_2FeP_2O_7$/C	$FeSO_4 \cdot 7H_2O$ (Sigma-Aldrich, $\geq$ 99.0%), LiH_2PO_4 (Sigma-Aldrich, $\geq$ 99.0%) Methylcellulose (Dow, Methocel™, A4C)	As above	650°C, dwell time: 30 min; flowing Ar + 10%H_2 (flow rate $\sim$ 0.1 dm³ min⁻¹)
Li_2FeSiO_4/C	$Fe(NO_3)_3 \cdot 9H_2O$ (Alfa Aesar, $\geq$ 98.0%), Li_2CO_3 (Alfa Aesar, $\geq$ 99.0%), $Si(OC_2H_5)_4$–TEOS (Alfa Aesar, 99,9%), Methylcellulose (Dow, Methocel™, A4C)	As above	750°C, dwell time: 10 min, flowing Ar + 5%H_2 (flow rate $\sim$ 0.1 dm³ min⁻¹)
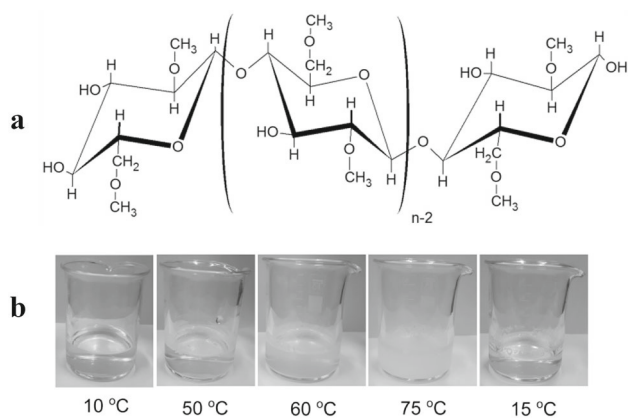
Figure 1. (**a**) Molecular structure of methylcellulose and (**b**) temperature dependence of methylcellulose' aqueous solubility.

125 Thanks to this ability of methylcellulose, we were able to
126 homogeneously mix the precursor compounds on a molec-
127 ular level and uniformly disperse them inside a methylcel-
128 lulose matrix. The methylcellulose thus serves as an
129 excellent gelating agent, which later on, in the second step,
130 pyrolytically degrades to carbon. The second step consists of
131 the following: the dried gel was grounded and then intro-
132 duced to a furnace at high temperature, later was kept for a
133 short duration of time in a flowing, slightly reducing atmo-
134 sphere (Ar + H_2) and then subsequently quenched to room
135 temperature. Duration of the heating step for Li_2FeSiO_4 and
136 $LiFePO_4$ samples was approximately 10 min. For $Li_2FeP_2O_7$
137 sample, the high-temperature dwell time had to be prolonged
138 to 30 min due to the substantial amount of impurities that
139 were obtained for the shorter periods of high-temperature
140 treatment (see supplementary data for more information).

141   The X-ray powder diffraction measurement was per-
142 formed on a Philips PW 1050 X-ray powder diffractometer
143 using Ni-filtered Cu Kα radiation and Bragg-Brentano
144 focusing geometry. The diffraction intensity was recorded
145 in the 2θ range of 10°–70° with a step size of 0.02° and a
146 counting time of 3 s per step. Powder Cell software was
147 used for determination of the constants of the lattice. The
148 microstructural parameters, namely the crystallite size and
149 the microstrain, were calculated based on the fundamental
150 parameters convolution approach to generate line profiles
151 [23] by using the XFIT-Koalariet software. Fityk program
152 was used for the deconvolution of X-ray diffraction (XRD)
153 profile to crystalline and amorphous part. The carbon con-
154 tent was determined thermogravimetrically. The morphol-
155 ogy of the synthesized powders was analysed by a field-
156 emission scanning electron microscope (FESEM, TESCAN,
157 MIRA3 XMU) at 20 kV. The particle size distributions
158 were determined by a laser-diffraction-based particle size
159 analyzer, Mastersizer 2000 (Malvern Instruments Ltd., UK).

160   The electrochemical measurements were conducted by
161 using Vertex. One potentiostat/galvanostat with an impe-
162 dance analyzer (Ivium Technologies). Cyclic voltammetry

163 (CV) measurements were performed in a three-electrode
164 cell with platinum as a counter and SCE (saturated calomel
165 electrode, SI Analytics) as a reference electrode; 6 M
166 solution of $LiNO_3$ (Alfa Aesar 99%) in H_2O was used as an
167 electrolyte. Chronopotentiometric (CP) measurements were
168 carried out in a closed, argon-filled two-electrode cell with
169 metallic Li as a counter electrode and 1 M solution of
170 $LiClO_4$ (Fluka, p.a.) in PC (propylene carbonate, Sigma-
171 Aldrich 99.7%) as an electrolyte. Working electrode for
172 both CP and CV measurements consisted of the active
173 material, carbon black and poly-vinylidenefluoride (PVDF,
174 Sigma-Aldrich) mixed in 85:10:5 weight ratio and depos-
175 ited on a platinum foil from the slurry prepared in
176 N-methyl-2-pyrrolidone (Sigma-Aldrich, 99%). Electro-
177 chemical impedance spectroscopy (EIS) was performed in
178 the frequency range from 10^5 to 10^{-2} Hz with an amplitude
179 of 5 mV and at open-circuit conditions of two-electrode cell
180 with the same setup as in CP measurements.

181 ## 3. Results and discussion

182 The presented gel-combustion procedure gives rise to
183 similar morphologies of the obtained powders, as
184 revealed by field emission scanning electron microscopy
185 (figure 2). The particles are agglomerated and irregular in
186 shape. Particle bonding and neck generation, indicating
187 inter-particle sintering, leads to a formation of irregularly
188 shaped pores of variable widths. The particle size distri-
189 butions have a lognormal shape (figure 2d) with close
190 span values of 1.09–1.27 (table 2). Distribution profiles of
191 Li_2FeSiO_4/C and $LiFePO_4$/C practically overlap each
192 other, while $Li_2FeP_2O_7$/C is a bit shifted in terms of
193 particle size and span.

194   The crystal phases of the synthesized powders were
195 confirmed by X-ray powder diffraction (figure 3). In
196 $LiFePO_4$/C sample, $LiFePO_4$ olivine phase (orthorhombic
197 space group no. 62, *Pnma*) was revealed along with the
198 traces of $Fe_2P_2O_7$ and Li_3PO_4 (altogether less than 5 wt%).
199 In Li_2FeSiO_4/C sample, Li_2FeSiO_4 phase crystallized in a
200 monoclinic space group no. 14 ($P2_1/c$), which corresponds
201 to the γ_s polymorph of the material [24]; besides the desired
202 phase, traces of Li_2SiO_3 were observed (< 2 wt%). In the
203 last sample, $Li_2FeP_2O_7$ phase crystallized within the same
204 space group no. 14 ($P2_1/c$) and was accompanied by the
205 olivine $LiFePO_4$ phase in the amount of 9–10 wt%.
206 Extended heat treatment (from 10 to 30 min) of the Li_2-
207 FeP_2O_7/C sample brought reduction of impurities, but not a
208 complete removal of olivine phase (supplementary data).
209 Since both phases are capable of Li intercalation and our
210 plan was to synthesize powders with significant
211 microstructural parameters, further prolongation of the heat
212 treatment was avoided. The creation of significant amount
213 of side products during synthesis of $Li_2FeP_2O_7$/C indicate,
214 however, a higher complexity, and thus slower kinetics of
215 formation of pyrophosphate $Li_2FeP_2O_7$ phase than olivine

LiFePO$_4$, although starting from the same precursor compounds (table 1).

The calculated unit cell parameters (table 2) are fairly consistent with earlier reports for the given phases. The obtained unit cell volumes are however slightly lower than in annealed powders (335.65 Å^3 for Li$_2$FeSiO$_4$ [25], 291.44 Å^3 for LiFePO$_4$ [16] and 1034.00 Å^3 for Li$_2$FeP$_2$O$_7$ [20]), which might be related to the significant quantity of strain that is observed (table 2). There was no evidence for the formation of crystalline carbon in the samples, therefore the internal non-graphitic carbon could be assumed to contribute to the background of XRD patterns. The amounts of the *in-situ*-formed carbon, established thermogravimetrically, were found to be 13, 10 and 8 wt% for Li$_2$FeSiO$_4$/C, LiFePO$_4$/C and Li$_2$FeP$_2$O$_7$/C, respectively. The crystallinity of a given sample was quantitatively estimated by resolving the diffraction intensity profile into contributions from the crystalline (sharp) diffractions and amorphous (diffuse) halo; the degree of crystallinity then equals the ratio of area of crystalline fraction to sum of areas of crystalline and amorphous fractions. The estimated values of crystallinity with regard to carbon content of the samples suggest that lattice distortions also contribute to the amorphous halo (table 2). The Li$_2$FeP$_2$O$_7$/C sample has somewhat higher degree of crystallinity, along with larger crystallite and particle size, probably due to the longer heat exposure. Because of the different chemistries involved, the comparisons from table 2 are not straightforward, but we can make some general comments: (a) fraction of amorphous phase, small crystallite size and notable microstrain confirm that the presented method yields powders with pronounced microstructural parameters; (b) in a given range of temperatures 650–750 °C, the dwell time had primary role to agglomeration and crystallite growth than temperature

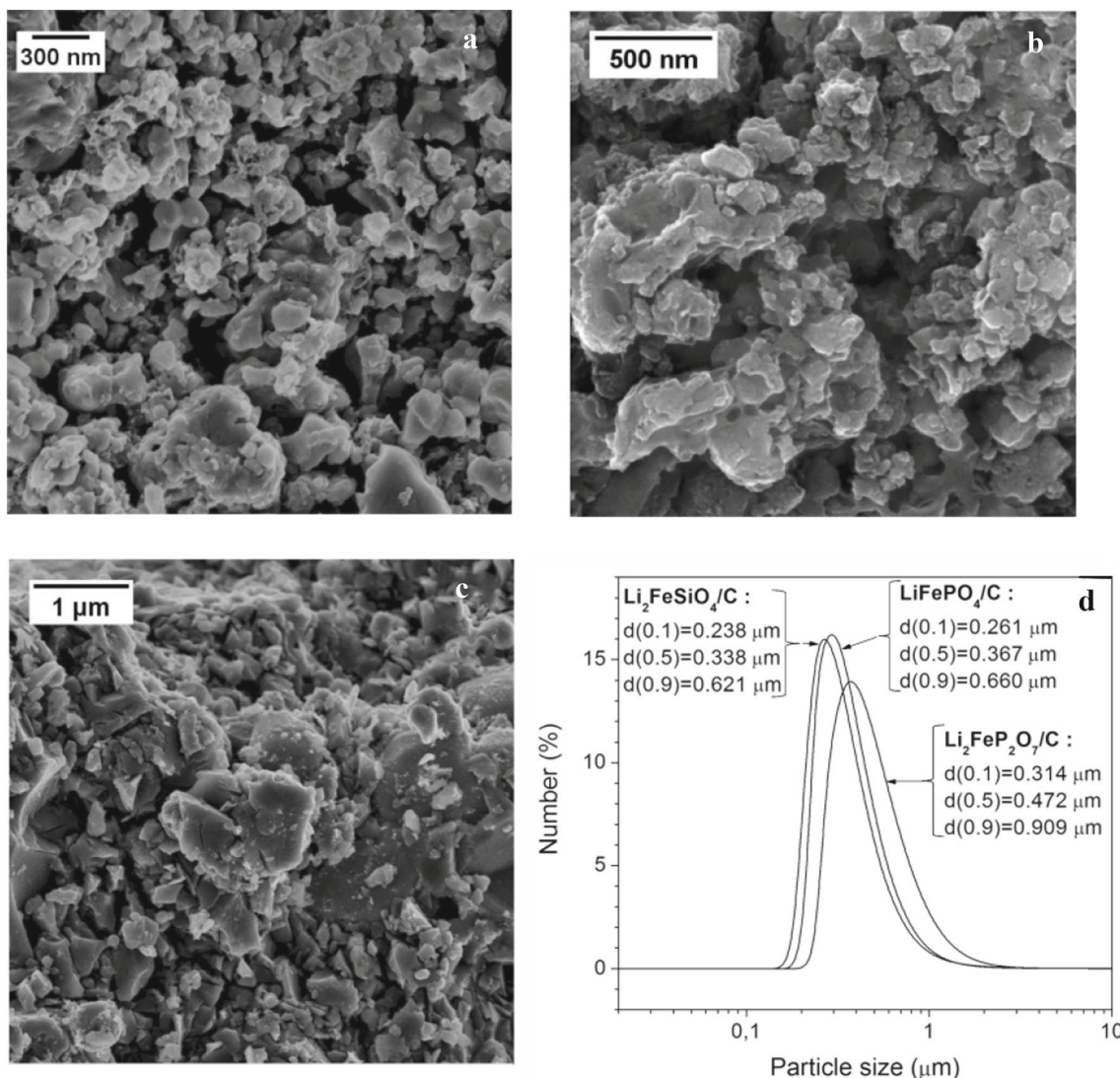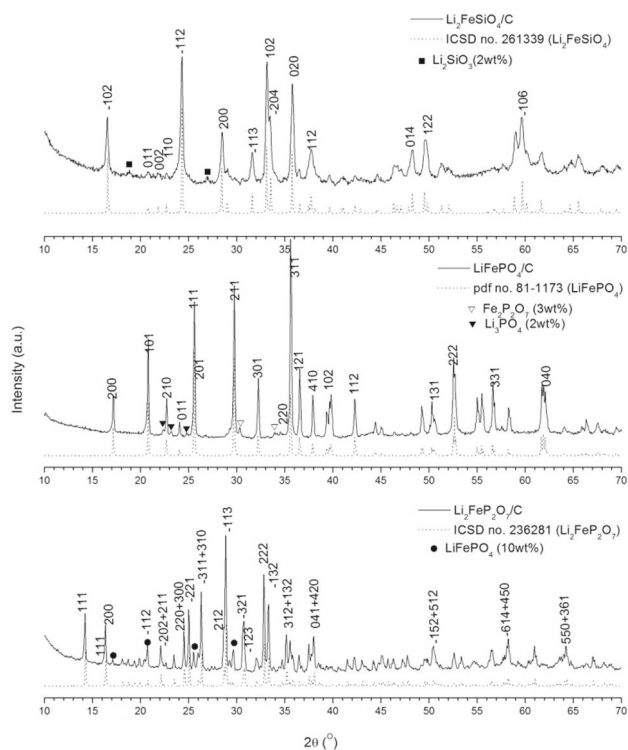**Figure 2.** SEM micrographs of (**a**) Li$_2$FeSiO$_4$/C, (**b**) LiFePO$_4$/C, (**c**) Li$_2$FeP$_2$O$_7$/C and (**d**) their particle size distributions.

Table 2. Structural and microstructural parameters of the prepared powders.

| Sample	Carbon content (wt%)	Lattice parameters		Crystallinity (%)	Mean crystallite size (nm)	Microstrain (%)	Mean particle size (μm)	Span*
Li_2FeSiO_4/C	13	$P2_1/c$	$a = 8.220$ Å	80	27	0.16	0.353	1.13
			$b = 5.008$ Å					
			$c = 10.690$ Å					
			$\beta = 130.475°$					
			$V = 334.767$ Å^3					
$LiFePO_4$/C	10	*Pnma*	$a = 10.325$ Å	87	46	0.20	0.367	1.09
			$b = 6.0053$ Å					
			$c = 4.691$ Å					
			$V = 290.884$ Å^3					
$Li_2FeP_2O_7$/C	8	$P2_1/c$	$a = 11.023$ Å	89	58	0.08	0.472	1.26
			$b = 9.756$ Å					
			$c = 9.807$ Å					
			$\beta = 101.545°$					
			$V = 1033.306$ Å^3					

*Span = {d(0.9) − d(0.1)}/d(0.5).

Figure 3. X-ray diffraction patterns of the obtained powders (solid line) and corresponding profiles taken from a crystallographic database (dotted line). The most prominent peaks are indexed in $P2_1/c$ (for Li_2FeSiO_4 and $Li_2FeP_2O_7$) and *Pnma* (LiFePO$_4$) symmetry group and observed impurity peaks are marked with a geometrically shaped signs.

value itself (see $Li_2FeP_2O_7$/C, which has the largest crystallites/particles although obtained at the lowest temperature, or Li_2FeSiO_4/C and LiFePO$_4$/C, which are obtained at different temperatures but with the same dwell time and both with similar particle size distributions); (c) the increase of carbon amount leads to a decrease of crystallite and particle size.

Redox behaviour of the synthesized polyanionic composites was first evaluated by the CV measurements in an aqueous electrolyte. All materials showed the electrochemical activity caused by the Fe^{3+}/Fe^{2+} redox pair. It can be observed from figure 4 that the redox process is strongly influenced by the chemical environment in a polyanion-based compound. When a FeO$_n$ polyhedron is coordinated with the $[SiO_4]^{4-}$ polyanions, the Fe^{3+}/Fe^{2+} redox process in Li-containing electrolyte is evidenced at − 0.55/− 0.32 V potentials *vs.* SCE at the scan rate of 10 mV s^{-1} (figure 4a). The amount of lithium (x) that can be reversibly removed upon this redox process may vary between 0 $< x < 1$, depending on the scan rate, since the removal of lithium above 1 occurs at higher potentials. The peak potential separation of 180 mV at 2 mV s^{-1} was found to be considerably smaller than that obtained for the carbon-coated Li_2FeSiO_4 (370 mV at 0.1 m Vs^{-1} in an aqueous electrolyte) prepared via citric acid-assisted method followed by 7 h thermal treatment [26]. It indicates faster charge transfer of our sample with approximately equal (13:14) carbon content, but prepared under rapid heating regime. However, the specific capacity of Li_2FeSiO_4/C sample measured galvanostatically in an organic electrolyte (see figure 6 below) was found to be comparable in the same voltage range to that obtained by the authors in [26],
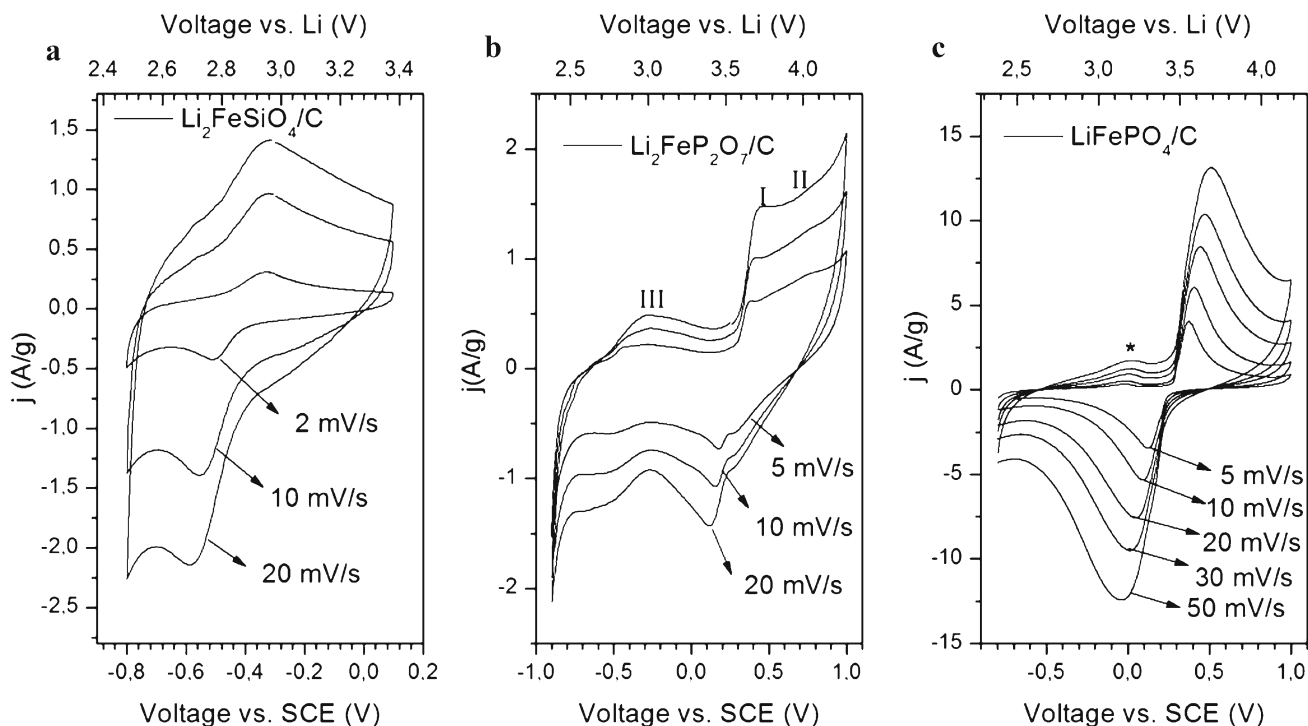
Figure 4. Cyclic voltammograms of the obtained composites at various scan rates; the potential *vs.* Li (top *x*-axis) is calculated from the measured potential *vs.* SCE (bottom *x*-axis) on the basis of reference tables of standard electrode potentials in aqueous solutions *vs.* normal hydrogen electrode [30].
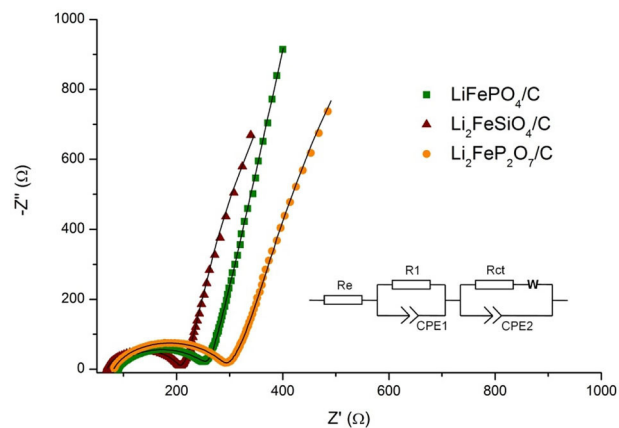
Figure 5. The Nyquist plots of the prepared two-electrode cells and the equivalent circuit scheme used in EIS analysis (inset).

282 which conveys that diffusion of Li^+ in the bulk of the
283 material is still a limiting factor for the intercalation
284 kinetics. The peak potential separation of the other two
285 samples is slightly higher ($\sim$ 240 mV in the given scan
286 rate) than that of Li_2FeSiO_4/C, which suggest higher
287 resistance of the charge transfer probably caused by the
288 lower amount carbon and larger crystallites/particles.
289   Due to the higher electronegativity of P *vs.* Si (inductive
290 effect), the redox potential of Fe^{3+}/Fe^{2+} is shifted towards a
291 more positive value in phosphates than in silicates, and due
292 to the increased electron delocalization in P_2O_7 (than in

293 PO_4) to even more positive values in pyrophosphate com-
294 pound [1]. One can see in figure 4b, the two main redox
295 peaks (labelled as I and II) of lithium iron pyrophosphate
296 are positioned at 0.16/0.39 and 0.28/0.69 V *vs.* SCE (10 mV
297 s^{-1}); these characteristic peaks, partially merged together
298 into a single broad peak, originate from Fe^{3+}/Fe^{2+} pair in
299 FeO_6 octahedral and FeO_5 bipyramidal coordination,
300 respectively [27]. There is, however, a third peak (III)
301 occurring at a lower potential of $-$ 0.55/$-$ 0.26 V *vs.* SCE
302 at 10 mV s^{-1}, which is not commonly seen in the literature
303 data of $Li_2FeP_2O_7$ (the small peak can be seen in [28], but it
304 is not commented). Interestingly, the occurrence of a similar
305 peak is observed for $Na_2FeP_2O_7$ phase and is prescribed to a
306 single-phase reaction of (de)sodiation, while the peaks at
307 higher potentials are related to the two-phase reactions [29];
308 the whole profile, although somewhat shifted, much
309 resembles our $Li_2FeP_2O_7$/C.
310   In figure 4c, one can notice characteristic redox peaks of
311 $LiFePO_4$ olivine phase, which correspond to the well-
312 known galvanostatic plateau at $\sim$ 3.4 V *vs.* Li. The current
313 response of $LiFePO_4$/C sample is significantly higher than
314 that measured for Li_2FeSiO_4/C and $Li_2FeP_2O_7$/C samples.
315 This indicates a significantly higher amount of stored
316 charge in olivine compared to other two samples under a
317 common current regime (note that a regular scan rates of
318 several mV s^{-1} in CV correspond to high current rates in
319 galvanostatic cycling, $> 1c$). An additional, small and broad
320 oxidation peak (marked with an asterisk) also appears at a

Table 3. The fitted kinetic parameters obtained from EIS.

Sample	R_e (Ω)	R_1 (Ω)	CPE1 (s^{N1} Ω^{-1})	N1	R_{ct} (Ω)	Z_w (Ω $s^{-1/2}$)	CPE2 (s^{N2} Ω^{-1})	N2
Li$_2$FeSiO$_4$/C	69.12	1.00×10^4	8.824×10^{-3}	0.98	135.5	34.8	7.919×10^{-6}	0.85
LiFePO$_4$/C	84.27	9.27×10^4	4.596×10^{-3}	0.93	173.9	15.7	3.592×10^{-5}	0.72
Li$_2$FeP$_2$O$_7$/C	81.61	1.18×10^4	2.146×10^{-2}	0.95	208.7	30.8	2.113×10^{-5}	0.79
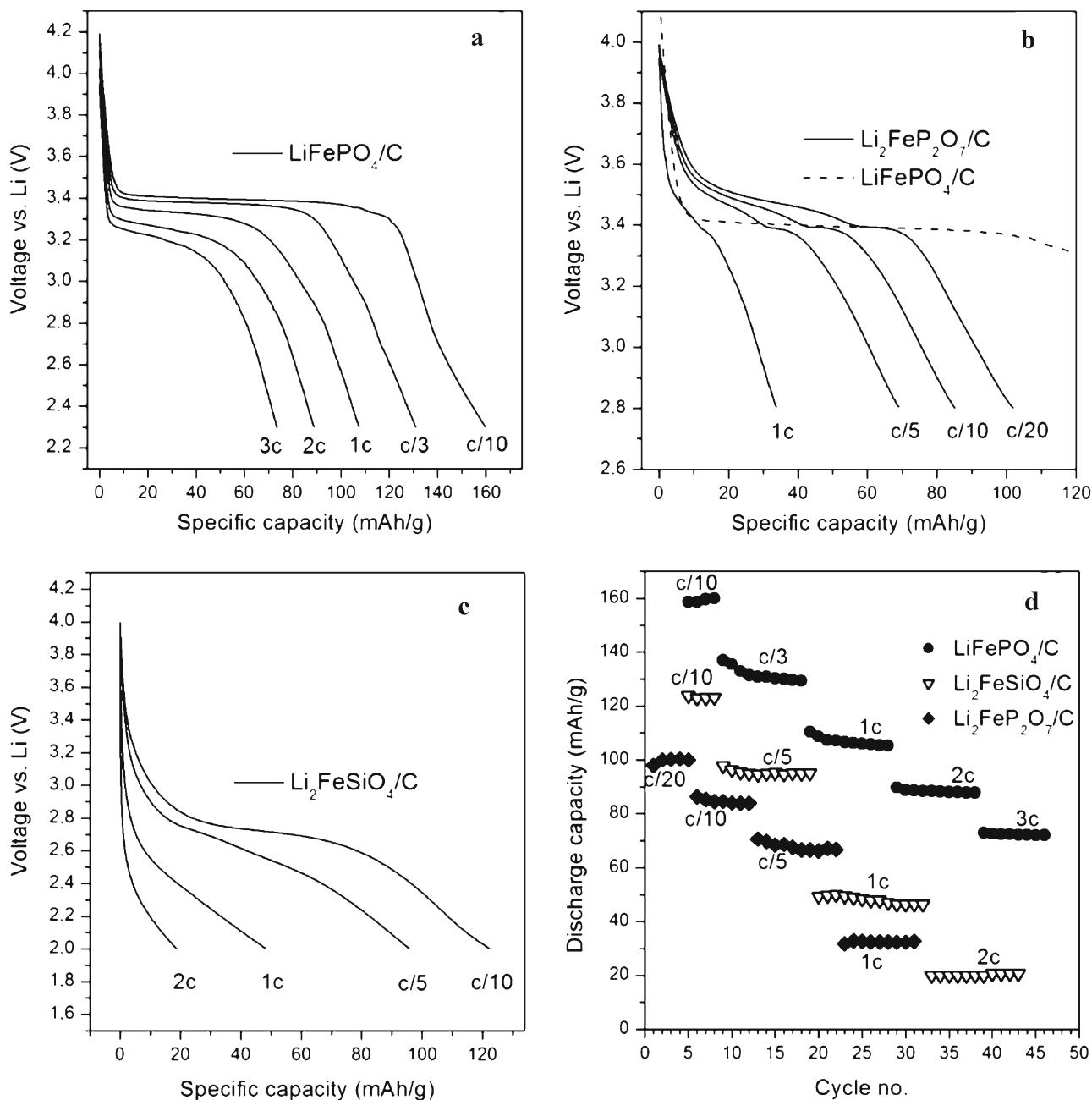
Figure 6. Discharge curves of the (**a**) LiFePO$_4$/C, (**b**) Li$_2$FeP$_2$O$_7$/C, (**c**) Li$_2$FeSiO$_4$/C and (**d**) their cycling performance.

potential of ≈ 0 V *vs*. SCE (10 mV s^{-1}), which can be attributed to the presence of the amorphous olivine phase [31]. Now, if we look back to our previous voltammogram (figure 4b) and take into consideration that amorphous olivine exhibits a single-phase reaction behaviour [10, 32], by analogy we could assume that the unknown peak (III) originates from amorphous $Li_2FeP_2O_7$, which would also be consistent with the reports regarding single-phase reaction of $Na_2FeP_2O_7$ [29].

After proved electrochemically both active and stable during CV measurements in aqueous electrolyte, the materials were tested as cathodes in Li-ion cell by galvanostatic charge–discharge tests in an organic electrolyte. Prior to galvanostatic tests, the assembled cells were examined by EIS at open circuit voltages. The impedance response is shown in figure 5. Each plot is composed of a depressed semicircle in the high-to-intermediate frequency region, followed by an inclined line at the lower frequencies. The impedance data were fitted with the equivalent circuit, shown in the inset of figure 5. The equivalent circuit model includes: (1) resistor R_e, which represents the sum of electrolyte resistance and the resistance of metallic contacts; (2) resistor R_1 paralleled with the constant phase element CPE1, which is related to the cathode composite and metal (Pt) current collector interface and/or solid electrolyte interface (SEI) film phenomena [33, 34]; (3) resistor R_{ct} paralleled with the constant phase element CPE2 and in serial with the general Warburg impedance Z_W, related to the cathode/electrolyte charge transfer resistance, double-layer capacitance and Li^+ solid-phase diffusion [35]. The inclusion of the constant phase elements, instead of pure capacitors, ensured a better fitting to the experimental data, as they better describe a real electrochemical system [34]. The charge transfer resistance of the tested electrode composites decreases in order $Li_2FeP_2O_7$/C > $LiFePO_4$/C > Li_2FeSiO_4/C (table 3), due to the reduction of crystallite/particle size and increase of conductive carbon concentration, both facilitating electron transfer. On the other hand, the lowest Warburg impedance for olivine composite indicates faster diffusion kinetics of this material.

The galvanostatic tests were performed at the room temperature in 4.0–2.8 V, 4.2–2.3 V and 4.0–2.0 V voltage range for $Li_2FeP_2O_7$/C, $LiFePO_4$/C and Li_2FeSiO_4/C composites, respectively. From the obtained chronopotentiometric curves at the given current rate, the specific capacities were calculated using the mass of the active material only (mass of carbon is subtracted from loading). The discharge curves along with the cycling performances are presented in figure 6. The current rates are given in *c/n* units, where *c* is a 1-electron theoretical capacity of the material (which is 166, 170 and 110 mAh g^{-1} for Li_2FeSiO_4, $LiFePO_4$ and $Li_2FeP_2O_7$, respectively) and *n* is a discharge time given in hours needed for a complete discharge. Discharge profile of $LiFePO_4$/C is distinguished by a flat plateau at around 3.4 V *vs*. Li (figure 6a), a mark of the two-phase process of lithium insertion/extraction reaction

[2]. On the other side, sloping curves of Li_2FeSiO_4/C and $Li_2FeP_2O_7$/C (figure 6b and c) suggest a monophasic reaction [36, 37]. Due to the presence of $LiFePO_4$ (rather than some phase transformations), the sloping curve of $Li_2FeP_2O_7$/C changes to a plateau at 3.4 V *vs*. Li (figure 6b), which makes this electrode a hybrid one. The materials were stable and performed reasonably well in accordance with its intrinsic capabilities. At low current densities, the capacities of 160 mAh g^{-1} (at *c*/10) for $LiFePO_4$/C, 124 mAh g^{-1} (*c*/10) for Li_2FeSiO_4/C and 101 mAh g^{-1} (*c*/20) for $Li_2FeP_2O_7$/C were obtained. Upon the increase of current rate, $LiFePO_4$/C powder exhibits the highest capacity preservation: 94% (at *c*/10), 80% (*c*/3), 65% (1*c*), 53% (2*c*) and 42% (3*c*). When compared to remarkable olivine, both $Li_2FeP_2O_7$/C and Li_2FeSiO_4/C show significantly lower performances (figure 6d). Although low in nominal specific capacity (due to the high molar mass of $Li_2FeP_2O_7$), the $Li_2FeP_2O_7$/C exhibits 92% utilization of its theoretical capacity at low current density. At different current rates, both $Li_2FeP_2O_7$/C and Li_2FeSiO_4/C utilize 75–77% (*c*/10), 60–63% (*c*/5) and 29–31% (1*c*) of its theoretical capacities. The capacity retention at the given rate was high for all the materials.

4. Conclusions

The polyanion cathode material's composites with carbon, namely, $LiFePO_4$/C, $Li_2FeP_2O_7$/C and Li_2FeSiO_4/C, were obtained by performing the experiments under extreme conditions of rapid heating, short high-temperature dwell and quenching to room temperature. A methylcellulose, water-soluble derivative of cellulose, was used as a polymer medium and a carbon source. The composites that were obtained have reduced crystallinity, with low crystallite size (20–60 nm) and significant microstrain (0.1–0.2). They provided stable electrochemical performance in both aqueous and organic electrolyte. The presence of amorphous phase induced spreading of existing peaks and/or the emergence of new broad peaks in CV. $LiFePO_4$/C powder exhibited superb electrode performance when compared to the $Li_2FeP_2O_7$/C and Li_2FeSiO_4/C samples. It manifests in significantly higher currents per gram provided in CV measurements and higher both capacity and capacity *vs*. current retention in galvanostatic charge–discharge tests. The potential application of Li_2FeSiO_4/C and $Li_2FeP_2O_7$/C composites thus may be limited to low power devices.

References

[1] Gutierrez A, Benedek N A and Manthiram A 2013 *Chem. Mater.* **25** 4010

[2] Padhi A K, Nanjundaswamy K S and Goodenough J B 1997 *J. Electrochem. Soc.* **144** 1188

[3] Nishimura S, Nakamura M, Natsui R and Yamada A 2010 *J. Am. Chem. Soc.* **132** 13596

[4] Nytén A, Abouimrane A, Armand M, Gustafsson T and Thomas J O 2005 *Electrochem. Commun.* **7** 156

[5] Zaghib K, Mauger A, Goodenough J B, Gendron F and Julien C M 2007 *Chem. Mater.* **19** 3740

[6] Zhang Y, Wang P, Zheng T, Li D, Li G and Yue Y 2018 *Nano Energy* **49** 596

[7] Xiong F, An Q, Xia L, Zhao Y, Mai L, Tao H *et al* 2019 *Nano Energy* **57** 608

[8] Guo H, Song X, Zhuo Z, Hu J, Liu T, Duan Y *et al* 2016 *Nano Lett.* **16** 601

[9] Gibot P, Casas-Cabanas M, Laffont L, Levasseur S, Carlach P, Hamelet S *et al* 2008 *Nat. Mater.* **7** 741

[10] Amisse R, Sougrati M T, Stievano L, Davoisne C, Dražič G, Budič B *et al* 2015 *Chem. Mater.* **27** 4261

[11] Hoang K and Johannes M 2011 *Chem. Mater.* **23** 3003

[12] Jensen K M Ø, Christensen M, Gunnlaugsson H P, Lock N, Bøjesen ED, Proffen T *et al* 2013 *Chem. Mater.* **25** 2282

[13] Jugović D, Milović M, Ivanovski V N, Avdeev M, Dominko R, Jokić B *et al* 2014 *J. Power Sources* **265** 75

[14] Dabas P and Hariharan K 2014 *RSC Adv.* **4** 14348

[15] Ferrari S, Capsoni D, Casino S, Destro M, Gerbaldi C and Bini M 2014 *Phys. Chem. Chem. Phys.* **16** 10353

[16] Jugović D, Mitrić M, Milović M, Cvjetićanin N, Jokić B, Umićević A *et al* 2017 *Ceram. Int.* **43** 3224

[17] Cyster L A, Grant D M, Howdle S M, Rose F R A J, Irvine D J, Freeman D *et al* 2005 *Biomaterials* **26** 697

[18] Li Y, Guo Z, Hao J and Ren S 2008 *J. Mater.* **208** 457

[19] Kotobuki M, Mizuno Y, Munakata H and Kanamura K 2011 *Electrochemistry* **79** 467

[20] Jugović D, Mitrić M, Milović M, Ivanovski V N, Škapin S, Dojčinović B *et al* 2019 *J. Alloys Compd.* **786** 912

[21] Milović M, Jugović D, Mitrić M, Dominko R, Stojković-Simatović I, Jokić B *et al* 2016 *Cellulose* **23** 239

[22] Takahashi M, Shimazaki M and Yamamoto J 2001 *J. Polym. Sci. Phys.* **39** 91

[23] Cheary R W and Coelho A 1992 *J. Appl. Crystallogr.* **25** 109

[24] Islam M S, Dominko R, Masquelier C, Sirisopanaporn C, Armstrong A R and Bruce P G 2011 *J. Mater. Chem.* **21** 9811

[25] Milović M D, Vasić Anićijević D D, Jugović D, Anićijević V J, Veselinović L, Mitrić M *et al* 2019 *Solid State Sci.* **87** 81

[26] Chen W, Lan M, Zhu D, Ji C, Feng X, Yang C *et al* 2013 *J. Mater. Chem. A* **1** 10912

[27] Kosova N V, Tsapina A M, Slobodyuk A B and Petrov S A 2015 *Electrochim. Acta* **174** 1278

[28] Zhang B, Ou X, Zheng J, Shen C, Ming L, Han Y *et al* 2014 *Electrochim. Acta* **133** 1

[29] Kim H, Shakoor R A, Park C, Lim S Y, Kim J S, Jo Y N *et al* 2013 *Adv. Funct. Mater.* **23** 1147

[30] Bard A J and Faulkner L R 2001 *Electrochemical methods: fundamentals and applications* 2nd ed (New York, United States: Wiley)

[31] Kisu K, Iwama E, Naoi W, Simon P and Naoi K 2016 *Electrochem. Commun.* **72** 10

[32] Naoi K, Kisu K, Iwama E, Nakashima S, Sakai Y, Orikasa Y *et al* 2016 *Energy Environ. Sci.* **9** 2143

[33] Gaberscek M, Moskon J, Erjavec B, Dominko R and Jamnik J 2008 *Electrochem. Solid State Lett.* **11** A170

[34] Schmidt J P, Chrobak T, Ender M, Illig J, Klotz D and Ivers-Tiffée E 2011 *J. Power Sources* **196** 5342

[35] Atebamba J -M, Moskon J, Pejovnik S and Gaberscek M 2010 *J. Electrochem. Soc.* **157** A1218

[36] Lu X, Wei H, Chiu H C, Gauvin R, Hovington P, Guerfi A *et al* 2015 *Sci. Rep.* **5** 1

[37] Shimizu D, Nishimura S, Barpanda P and Yamada A 2012 *Chem. Mater.* **24** 2598